

# Optimized Diagonal and Pseudo-random Phase Precoding Schemes for MIMO VLC Systems

Ashok D. R. and A. Chockalingam

Department of ECE, Indian Institute of Science, Bangalore 560012

**Abstract**—Dual-LED complex modulation (DCM) and quad-LED complex modulation (QCM) are state-of-the-art MIMO modulation schemes which efficiently transmit complex-valued modulation symbols in visible light communication (VLC). DCM uses two LEDs to transmit complex symbols exploiting their polar form of representation. QCM uses four LEDs to transmit complex symbols through intensity modulation to convey the magnitude of real and imaginary parts of a complex symbol and spatial modulation to convey the sign information. In this paper, we introduce efficient precoding schemes for DCM and QCM schemes. The first proposed precoder is for DCM, and it is termed as *optimized diagonally precoded DCM (ODP-DCM)*. In ODP-DCM, the magnitude and phase information are weighted such that the normalized minimum distance is maximized. The second precoder is for both DCM and QCM, and it is termed as *pseudo-random phase precoded DCM/QCM (PRPP-DCM/QCM)*. In PRPP-DCM/QCM, pseudo-random phase matrices which do not need any channel knowledge at the transmitter for their construction are used as the precoding matrices. Numerical results show that the proposed precoding schemes achieve good performance and alleviate the effect of spatial correlation in MIMO VLC channels.

**Keywords** – Visible light communication, MIMO VLC systems, MIMO modulation schemes, DCM, QCM, precoding schemes.

## I. INTRODUCTION

Visible light communication (VLC) systems are increasingly getting recognized as an attractive technology for wireless communications in indoor and vehicular environments [1]. One of the key advantages of VLC systems is that the VLC transceivers are simple and low cost. Commercially available lighting LEDs (light emitting diodes) and photodiodes (PD) serve as optical wireless transmitters and receivers, respectively [2]. VLC systems are particularly attractive for indoor applications because of their ability to provide lighting and short-range wireless connectivity simultaneously. In closed-room applications, VLC systems can provide inherent security as well. Spectrum at no cost and no licensing issues are other advantages of VLC. In VLC, information is carried through optical intensity radiated by the transmit LED. Therefore, the information signals that intensity modulate the LED must be real and non-negative.

As in RF wireless communications, multiple-input and multiple output (MIMO) techniques can offer rate and performance benefits in VLC systems as well [3],[4]. Among the modulation schemes suited for MIMO VLC, SMP, SSK, SM, and their variants have been popularly studied in MIMO VLC systems [5]-[7]. Two issues need attention in MIMO VLC systems. One is the ability to carry complex modulation symbols in MIMO VLC channels, and the other is the need to address the degrading effect of the high degree of spatial correlation present in MIMO VLC channels.

This work was supported in part by the J. C. Bose National Fellowship, Department of Science and Technology, Government of India.

The first issue is popularly addressed through Hermitian symmetry operation, followed by a bipolar to unipolar conversion operation [8]. A more recent approach to address the first issue is to use multiple LEDs and exploit the spatial domain to transmit complex symbols, thereby avoiding the Hermitian symmetry and unipolar conversion operations. *Quad-LED complex modulation* (QCM) and *Dual-LED complex modulation* (DCM) are two modulation schemes that use this approach [9],[10]. DCM uses two LEDs to transmit complex symbols exploiting their polar form of representation. QCM uses four LEDs to transmit complex symbols through intensity modulation to convey the magnitude of real and imaginary parts of a complex symbol and spatial modulation to convey the sign information. It has been shown that DCM and QCM can achieve better performance compared to other popular MIMO modulation schemes such as spatial multiplexing (SMP) [9],[10].

One approach to address the second issue is to provide the receiver with an imaging lens [11],[12]. While imaging lens is a fix at the receiver side, precoding can serve as a fix at the transmit side. We, in this paper, focus on the precoding approach on the transmit side. In particular, we propose two efficient precoding schemes for point-to-point MIMO VLC systems that employ DCM and QCM schemes. While precoding schemes in multiuser MIMO VLC systems on the downlink have been studied in the literature [13],[14], the MIMO VLC precoding schemes we propose for DCM and QCM have not been reported. Our contributions in this paper can be summarized as follows. We introduce two efficient MIMO-VLC precoding schemes. The first proposed precoder is for DCM, and it is termed as *optimized diagonally precoded DCM (ODP-DCM)*. In ODP-DCM, the magnitude and phase information are weighted such that the normalized minimum distance is maximized. The second precoder is for both DCM and QCM, and it is termed as *pseudo-random phase precoded DCM/QCM (PRPP-DCM/QCM)*. In PRPP-DCM/QCM, pseudo-random phase matrices which do not need any channel state information at the transmitter (CSIT) for their construction are used as the precoding matrices. The proposed precoding schemes achieve good performance and alleviate the effect of spatial correlation in MIMO VLC channels.

## II. INDOOR MIMO VLC SYSTEM MODEL AND COMPLEX MODULATION SCHEMES

### A. Indoor MIMO VLC system model

Consider an indoor MIMO VLC system with  $N_t$  LEDs (transmitter) and  $N_r$  PDs (receiver), where the LEDs are assumed to have Lambertian radiation pattern [15]. The LEDs and the PDs are placed in a room of size  $5m \times 5m \times 3.5m$  as shown in Fig. 1. The LEDs are placed 0.5m below the ceiling

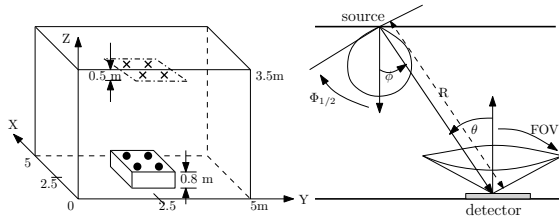


Fig. 1. Geometric set-up of the considered indoor VLC system. A dot represents a photo detector and a cross represents an LED.

and the PDs are placed on a table of height 0.8m. Let  $d_{tx}$  denote the spacing between the LEDs and  $d_{rx}$  denote the spacing between the PDs. In a given signaling interval, an LED is either OFF or emits light with some intensity. Let  $\mathbf{x} = [x_1 \ x_2 \ \cdots \ x_{N_t}]^T$  be the  $N_t \times 1$  transmit vector, where  $x_i$  is the light intensity emitted by the  $i$ th LED. The MIMO VLC channel matrix  $\mathbf{H}$  is of the order  $N_r \times N_t$  and its  $(i, j)$ th element  $h_{ij}$  is the path gain from the  $j$ th LED to the  $i$ th PD,  $j = 1, \dots, N_t$ , and  $i = 1, \dots, N_r$ . The LOS path gain  $h_{ij}$  is given by [15]

$$h_{ij} = \frac{n+1}{2\pi} \cos^n \phi_{ij} \cos \theta_{ij} \frac{A}{R_{ij}^2} \text{rect}\left(\frac{\theta_{ij}}{\text{FOV}}\right), \quad (1)$$

where  $\phi_{ij}$  is the angle of emergence from the  $j$ th source (LED) with respect to the normal at the source,  $n$  is the mode number of the radiating lobe which is given by  $n = \frac{-\ln(2)}{\ln \cos \Phi_{1/2}}$ ,  $\Phi_{1/2}$  is the half-power semiangle of the LED,  $\theta_{ij}$  is the angle of incidence at the  $i$ th PD,  $A$  is the area of the PD,  $R_{ij}$  is the distance between the  $j$ th LED and the  $i$ th PD, FOV is the field-of-view of the PD, and  $\text{rect}(x) = 1$ , if  $|x| \leq 1$ , and  $\text{rect}(x) = 0$ , if  $|x| > 1$ . See Fig. 1 for the definition of various angles in the model. The  $N_r \times 1$  received signal vector at the receiver in the electrical domain is given by

$$\mathbf{y} = a\mathbf{H}\mathbf{x} + \mathbf{n}, \quad (2)$$

where  $a$  is the responsivity of the PD (in Amperes/Watt) and  $\mathbf{n} = [n_1 \ n_2 \ \cdots \ n_{N_r}]^T$  is the noise vector. The optical intensity values of the  $x_i$ s in  $\mathbf{x}$  are determined by the modulation scheme used. The electrical-to-optical conversion factor at the transmitter is assumed to be unity. The optical-to-electrical conversion factor at the receiver is given by the responsivity  $a$  Amp/Watt. The electrical noise  $n_i$ s in  $\mathbf{n}$  are modeled as i.i.d. real AWGN with zero mean and variance  $\sigma^2$ . The SNR at a PD in the electrical domain is defined as  $\frac{(aP_r)^2}{\sigma^2}$ , where  $P_r$  is the total received optical power and  $\sigma^2$  is the total noise power at a PD. The total power received at the  $i$ th PD is given by  $(\mathbf{H}_i\mathbf{x})^2$ . Therefore, the average received optical power is given by  $\mathbb{E}\{\|\mathbf{H}\mathbf{x}\|^2\} = \frac{1}{N_r} \sum_{i=1}^{N_r} \mathbb{E}\{(\mathbf{H}_i\mathbf{x})^2\}$ , where  $\mathbf{H}_i$  is the  $i$ th row of  $\mathbf{H}$ ,  $\|\cdot\|$  is the Euclidean norm operator,  $\mathbb{E}\{\cdot\}$  is the expectation operator, and the expectation is w.r.t. the signal vector  $\mathbf{x}$ . Hence, the average SNR at the receiver in the electrical domain is given by  $\bar{\gamma} = \frac{a^2}{\sigma^2 N_r} \sum_{i=1}^{N_r} \mathbb{E}\{(\mathbf{H}_i\mathbf{x})^2\}$ , and the corresponding  $E_b/N_0$  is given by  $E_b/N_0 = \frac{\bar{\gamma}}{\eta}$ , where  $\eta$  is the rate of the modulation scheme in bits per channel use (bpcu). The various system parameters considered in this paper are presented in Table I.

Room	Dimension ( $X \times Y \times Z$ )	$5m \times 5m \times 3.5m$
Transmitter	No. of LEDs ( $N_t$ )	DCM: 2; QCM: 4
	Height from the floor	3m
	$\Phi_{1/2}$	$60^\circ$
	Mode number, $n$	1
	$d_{tx}$	0.2m to 4.8m
Receiver	No. of PDs ( $N_r$ )	4
	Height from the floor	0.8m
	Responsivity, $a$	0.4 Ampere/Watt
	FOV	$85^\circ$
	$d_{rx}$	0.1m

TABLE I  
SYSTEM PARAMETERS IN THE CONSIDERED INDOOR VLC SYSTEM.

### B. DCM transmitter

The DCM scheme uses two LEDs for transmission. A symbol from a complex alphabet  $\mathbb{A}$  (e.g., QAM) is chosen based on  $\log_2 |\mathbb{A}|$  information bits. For the chosen complex symbol  $s \in \mathbb{A}$ , the DCM transmit vector  $\mathbf{x}$  is obtained as follows:

$$r = |s|, \quad r \in \mathbb{R}^+; \quad \phi = \arg(s), \quad \phi \in [0, 2\pi) \\ \mathbf{x} = [\phi \ r]^T. \quad (3)$$

That is, one of the LED emits intensity  $\phi$  and the other one emits intensity  $r$ .

### C. QCM transmitter

The QCM scheme uses four LEDs at the transmitter. A symbol from a complex alphabet  $\mathbb{A}$  is chosen based on  $\log_2 |\mathbb{A}|$  bits. For the chosen complex symbol  $s \in \mathbb{A}$ , the QCM transmit vector  $\mathbf{x}$  is obtained as follows :

$$x_1 = 0.5|s_I|(1 + \text{sgn}(s_I)), \quad x_2 = 0.5|s_I|(1 - \text{sgn}(s_I)), \\ x_3 = 0.5|s_Q|(1 + \text{sgn}(s_Q)), \quad x_4 = 0.5|s_Q|(1 - \text{sgn}(s_Q)), \\ \mathbf{x} = [x_1 \ x_2 \ x_3 \ x_4]^T, \quad (4)$$

where  $s_I$  and  $s_Q$  are the real and imaginary parts of  $s$ , respectively, and  $\text{sgn}(z) = 1$  if  $z > 0$ ,  $\text{sgn}(z) = -1$  if  $z < 0$ , and  $\text{sgn}(z) = 0$  if  $z = 0$ . The intensity values  $x_1$ ,  $x_2$ ,  $x_3$ , and  $x_4$  are radiated using four LEDs. Note that, in a given channel use, only two elements in  $\mathbf{x}$  will be non-zero (i.e., the corresponding LEDs will be active) and the other two will be zero (the corresponding LEDs will be inactive). The intensities on the active (ON) LEDs convey the magnitudes of  $s_I$  and  $s_Q$ , and their sign information is conveyed by which LEDs are active (ON)/inactive (OFF).

### D. DCM/QCM signal detection

The maximum-likelihood (ML) estimate of the transmit vector  $\mathbf{x}$  is obtained as

$$\hat{\mathbf{x}}_{\text{ML}} = \underset{\mathbf{x} \in \mathbb{S}}{\text{argmin}} \|\mathbf{y} - a\mathbf{H}\mathbf{x}\|^2, \quad (5)$$

where  $\mathbb{S}$  denotes the DCM/QCM signal set (i.e., set of all possible DCM/QCM  $\mathbf{x}$  vectors). The detected vector  $\hat{\mathbf{x}}_{\text{ML}}$  is demapped back to the corresponding complex symbol  $\hat{s}_{\text{ML}}$ , which is further demapped to get the corresponding information bits.

### III. OPTIMIZED DIAGONALLY PRECODED DCM

In this proposed precoding scheme, the transmit vector is  $\mathbf{W}\mathbf{x}$ , where  $\mathbf{x}$  is a DCM signal vector and  $\mathbf{W}$  is a  $2 \times 2$  diagonal precoder matrix. Let  $\mathbf{W} = \text{diag}(w_1, w_2)$ ,  $w_1, w_2 \in \mathbb{R}_{\geq 0}$ . Restricting  $w_1$  and  $w_2$  to be strictly positive, the precoder matrix can be written as

$$\mathbf{W} = w_1 \mathbf{W}_k, \quad (6)$$

where  $\mathbf{W}_k = \text{diag}(1, k)$ ,  $k = w_2/w_1$ ,  $k > 0$ . The average transmit optical power ( $P_t$ ) contributed by both the LEDs is given by

$$P_t = w_1(\phi_{avg} + k r_{avg}), \quad (7)$$

where  $\phi_{avg} = \mathbb{E}[\phi]$  and  $r_{avg} = \mathbb{E}[r]$ . Using (7), (6) can be written as

$$\mathbf{W} = \left( \frac{P_t}{\phi_{avg} + k r_{avg}} \right) \mathbf{W}_k. \quad (8)$$

Now, the received vector for this scheme can be written as

$$\begin{aligned} \mathbf{y} &= a\mathbf{H}\mathbf{W}\mathbf{x} + \mathbf{n} \\ &= a \left( \frac{P_t}{\phi_{avg} + k r_{avg}} \right) \mathbf{H}\mathbf{W}_k \mathbf{x} + \mathbf{n}. \end{aligned} \quad (9)$$

Fixing  $P_t$  based on power constraint at the transmitter, we can vary  $k$ . When  $k \ll 1$ , most of the power is used for the phase information  $\phi$ . As  $k$  increases, the power distribution becomes more favorable to magnitude information  $r$ . We look for the  $k$  which gives the best asymptotic BER performance. Towards that, consider the normalized minimum distance of the received signal set, defined as

$$\tilde{d}_{min,\mathbf{H}} = \min_{\mathbf{z}_i, \mathbf{z}_j \in \hat{\mathbb{S}}_R} \|\mathbf{z}_i - \mathbf{z}_j\|, \quad (10)$$

where  $\hat{\mathbb{S}}_R = \{\mathbf{z}_1, \mathbf{z}_2 \dots \mathbf{z}_N\}$  denotes the set of normalized noiseless received signal vectors, where  $\mathbf{z}_i$  is given by

$$\mathbf{z}_i = \frac{\mathbf{y}_i}{\sqrt{\frac{1}{NN_r} \sum_{j=1}^N \|\mathbf{y}_j\|^2}}, \quad (11)$$

where  $\mathbf{y}_i$  is the noiseless received signal vector when the transmit vector is  $\mathbf{W}\mathbf{x}_i$ , and  $\{\mathbf{x}_1, \mathbf{x}_2 \dots \mathbf{x}_N\}$  is DCM signal set, i.e.,  $\mathbf{y}_i = a\mathbf{H}\mathbf{W}\mathbf{x}_i$ . Now, (11) can be written as

$$\mathbf{z}_i = \frac{\mathbf{H}\mathbf{W}_k \mathbf{x}_i}{\sqrt{\frac{1}{NN_r} \sum_{j=1}^N \|\mathbf{H}\mathbf{W}_k \mathbf{x}_j\|^2}}. \quad (12)$$

We choose the optimum  $k$  as

$$k_{opt} = \underset{k}{\text{argmax}} \tilde{d}_{min,\mathbf{H}}. \quad (13)$$

In order to illustrate the  $\tilde{d}_{min,\mathbf{H}}$  versus  $k$  characteristics of the proposed diagonally precoded DCM scheme, we numerically computed  $\tilde{d}_{min,\mathbf{H}}$  as a function of  $k$  for 16-QAM considering the indoor VLC system shown in Fig. 1 with system parameters as in Table I with  $d_{tx} = 1$ m. The results are plotted in Fig. 2. From Fig. 2, we observe that  $d_{min,\mathbf{H}}$  takes its maximum value at  $k = 0.1$ , i.e.,  $k_{opt}$  as per (13) is 0.1 and the maximum  $\tilde{d}_{min,\mathbf{H}}$  is about 0.145. We call the diagonally precoded DCM that uses  $k = k_{opt}$  in the precoder as ‘optimized diagonally precoded DCM’ (ODP-DCM). Using the  $k_{opt}$  value in the precoder essentially minimizes the BER in the high SNR regime. We illustrate the BER performance achieved by the ODP-DCM scheme next.

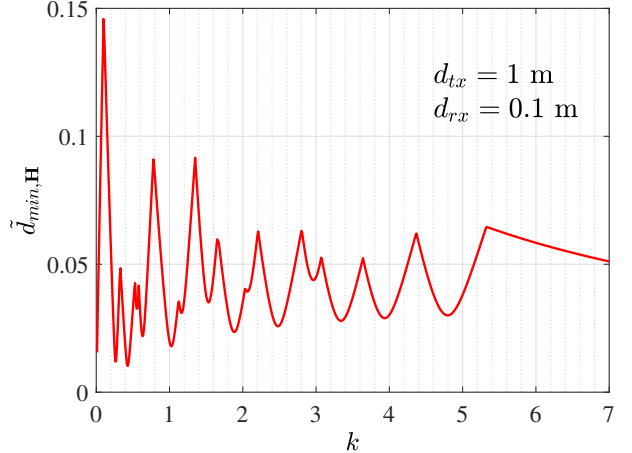


Fig. 2. Plot of  $\tilde{d}_{min,\mathbf{H}}$  as a function of  $k$  for diagonally precoded DCM(16-QAM).

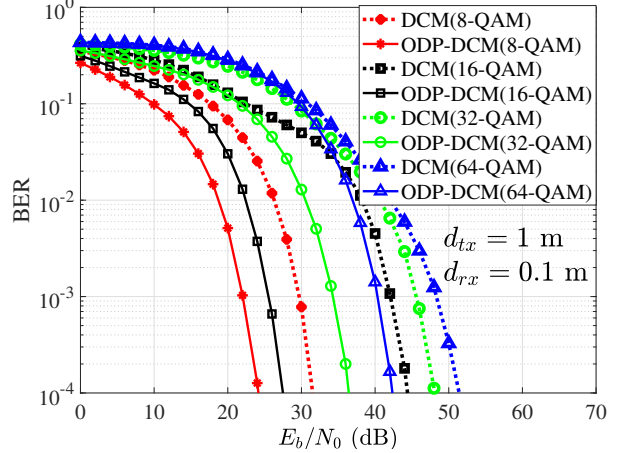


Fig. 3. BER performance of DCM and ODP-DCM for different QAM constellations.

#### A. BER performance of ODP-DCM

In Fig. 3, we plot the simulated BER performance of the proposed ODP-DCM scheme and the DCM scheme without precoding for the cases of 8-QAM, 16-QAM, 32-QAM, and 64-QAM having the system parameters in Table I with  $d_{tx} = 1$ m. We can see that DCM with the proposed optimized precoding achieves significantly better BER compared to DCM without precoding. For example, the proposed ODP-DCM achieves SNR gains of about 16 dB and 12 dB at  $10^{-4}$  BER compared to DCM without precoding for the cases of 16-QAM and 32-QAM, respectively. We further note that these SNR gains are well captured analytically by the asymptotic (noiseless) metric  $\tilde{d}_{min,\mathbf{H}}$ . To illustrate this, in Fig. 4, we plot  $20 \log(\tilde{d}_{min})$  as a function of  $d_{tx}$  for the proposed ODP-DCM scheme as well as the DCM scheme without precoding for 16-QAM and 32-QAM. We can see in this figure that, at  $d_{tx} = 1$ m, the gap between the DCM (32-QAM) curve and the ODP-DCM (32-QAM) curve is about 12 dB, which is the same as the SNR gain observed in Fig. 3 for 32-QAM. Likewise, the gap between the DCM (16-QAM) curve and the ODP-DCM (16-QAM) curve in Fig. 4 at  $d_{tx} = 1$ m is about 16 dB, which also corroborates with the SNR gain observed in Fig. 3 for 16-QAM.

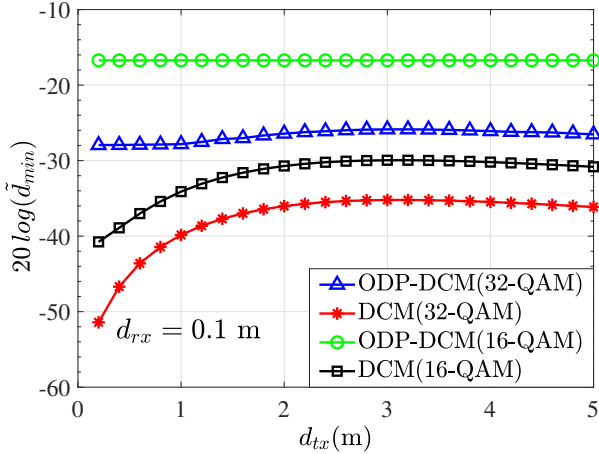


Fig. 4. Variation of normalized minimum distance of the proposed ODP-DCM and DCM as a function of  $d_{tx}$  for 16/32-QAM.

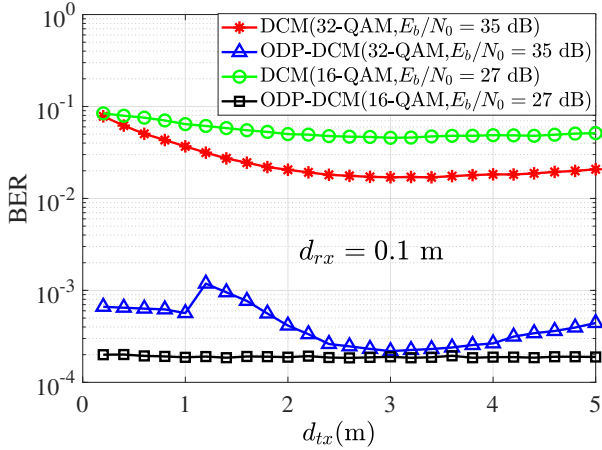


Fig. 5. BER performance of DCM and ODP-DCM as a function of  $d_{tx}$  for 16/32-QAM.

#### B. Effect of varying $d_{tx}$ on ODP-DCM performance

Next, in Fig. 5, we show the BER performance of ODP-DCM and DCM without precoding as a function of  $d_{tx}$  for 16-QAM and 32-QAM at  $E_b/N_0 = 27$  dB and 35 dB. It is observed that ODP-DCM achieves very good performance compared to DCM even for low  $d_{tx}$  values. For example, at  $d_{tx} = 0.2$ m, there is a two order improvement in BER. Asymptotically the behaviour of varying  $d_{tx}$  can be observed clearly from Fig.4. The SNR gain due to the proposed precoding compared to no precoding is more for smaller values of  $d_{tx}$  where the spatial correlation will be high. For example, at  $d_{tx} = 0.2$ m, ODP-DCM has 26 dB SNR gain over DCM without precoding for 16-QAM and 24 dB gain for 32-QAM. Thus the optimized precoder significantly alleviates the degrading effect of spatial correlation in MIMO VLC channels.

#### IV. PRPP FOR DCM AND QCM SCHEMES

In this section, we propose a precoding scheme which does not need any CSI at the transmitter. The scheme is suited for both DCM as well as QCM and is termed as ‘pseudo-random phase precoded DCM/QCM’ (PRPP-DCM/QCM) scheme.

##### A. PRPP-DCM/QCM scheme

In this precoding scheme, precoding is done before complex symbols are mapped to the transmit vector unlike in the di-

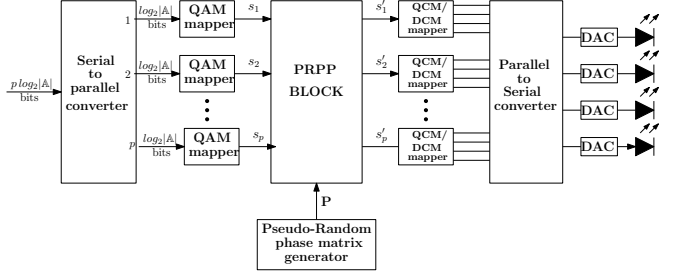


Fig. 6. PRPP-DCM/QCM transmitter.

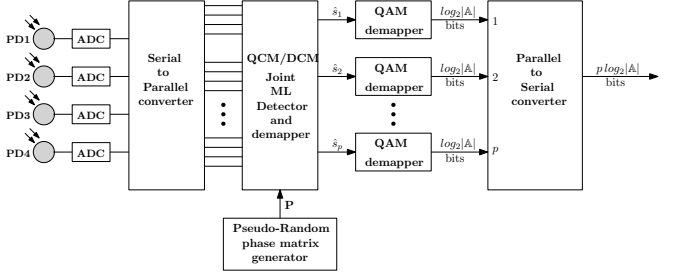


Fig. 7. PRPP-DCM/QCM receiver.

agonal precoder where precoding is done after mapping complex symbols to the transmit vector. The PRPP-DCM/QCM transmitter is shown in Fig. 6. In case of QCM all the four LEDs are used, whereas in case of DCM only two LEDs are used. The PRPP-DCM/QCM scheme sends  $p \log_2 |\mathbb{A}|$  bits in  $p$  channel uses, where  $\mathbb{A}$  is a conventional modulation alphabet (e.g., QAM). First,  $p \log_2 |\mathbb{A}|$  bits are mapped to a complex vector  $\mathbf{s} = [s_1 \ s_2 \ \dots \ s_p]^T$  which belongs to the set  $\mathbb{A}^p$ . This complex symbol vector is multiplied by a PRPP matrix  $\mathbf{P}$  to get the vector  $\mathbf{s}' = [s'_1 \ s'_2 \ \dots \ s'_p]^T$  as  $\mathbf{s}' = \mathbf{Ps}$ , where the PRPP matrix  $\mathbf{P}$  is of the order  $p \times p$  and the  $(l, m)$ th element of  $\mathbf{P}$  is  $e^{j\phi_{p(l-1)+m}}$ . The phases  $\phi_1, \phi_2, \dots, \phi_{p^2} \in [0, 2\pi]$  are generated by a pseudo-random generator based on some seed which is also available at the receiver [16]. The transmit vector which is transmitted in  $i$ th channel use ( $\mathbf{x}_i$ ) is obtained from the complex symbol  $s'_i$  based on QCM or DCM. The corresponding received vector at the receiver will be

$$\mathbf{y}_i = \mathbf{aHx}_i + \mathbf{n}_i. \quad (14)$$

The relation between transmit vectors and received vectors using (14) over  $p$  channel uses can be jointly written as

$$\mathbf{y} = \mathbf{a}(\mathbf{I}_p \otimes \mathbf{H})\mathbf{x} + \mathbf{n}, \quad (15)$$

where  $\mathbf{y} = [\mathbf{y}_1^T \ \mathbf{y}_2^T \ \dots \ \mathbf{y}_p^T]^T$ ,  $\mathbf{x} = [\mathbf{x}_1^T \ \mathbf{x}_2^T \ \dots \ \mathbf{x}_p^T]^T$ ,  $\mathbf{n} = [\mathbf{n}_1^T \ \mathbf{n}_2^T \ \dots \ \mathbf{n}_p^T]^T$  and  $\mathbf{I}_p$  is  $p \times p$  identity matrix. The set of all possible values of vector  $\mathbf{x}$  depends on the type of modulation (DCM/QCM) and the precoder matrix  $\mathbf{P}$ . Denoting it as  $\mathbb{S}_{\mathbf{P}}$  the joint ML-estimate of  $\mathbf{x}$  at the receiver will be

$$\hat{\mathbf{x}} = \underset{\mathbf{x} \in \mathbb{S}_{\mathbf{P}}}{\operatorname{argmin}} \|\mathbf{y} - \mathbf{a}(\mathbf{I}_p \otimes \mathbf{H})\mathbf{x}\|^2. \quad (16)$$

At the receiver the joint ML-estimate  $\hat{\mathbf{x}}$  over  $p$  channel use is computed and is split into the vectors  $\hat{\mathbf{x}}_1, \hat{\mathbf{x}}_2, \dots, \hat{\mathbf{x}}_p$ . These vectors are demapped to obtain complex symbol vector  $\hat{\mathbf{s}} = [\hat{s}_1 \ \hat{s}_2 \ \dots \ \hat{s}_p]$ , which is in turn demapped to obtain  $p \log_2 |\mathbb{A}|$  bits. The block diagram of PRPP-DCM/QCM receiver is shown in Fig. 7.

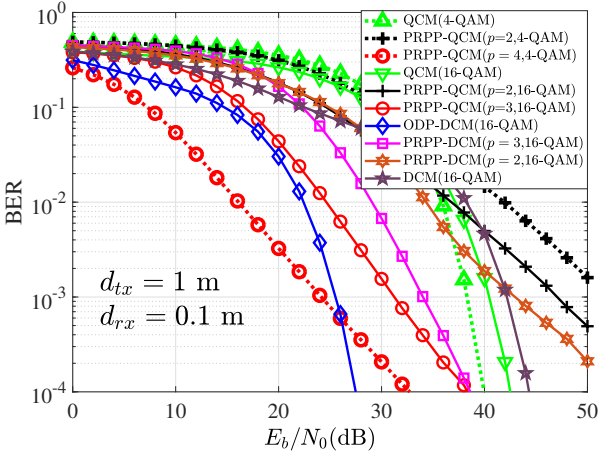


Fig. 8. BER performance of PRPP-DCM, ODP-DCM, DCM, PRPP-QCM, and QCM.

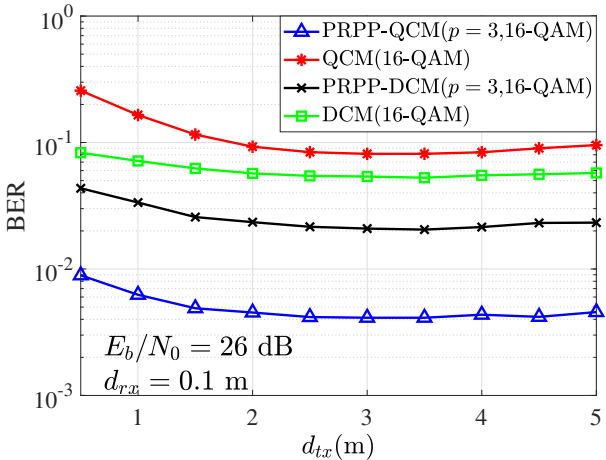


Fig. 9. BER performance of DCM, PRPP-DCM, QCM, and PRPP-QCM as a function of  $d_{tx}$ .

### B. BER performance of PRPP-DCM/QCM

In this subsection, we present the simulated BER performance of the proposed PRPP-DCM/QCM schemes. In Fig. 8, we present the BER performance of PRPP-DCM for the case of 16-QAM with  $p = 2, 3$ . The performance ODP-DCM and DCM without precoding are plotted for comparison. We observe that the performance of PRPP-DCM improves as  $p$  is increased (see the PRPP-DCM BER plots for  $p = 2$  and  $3$ ). For  $p = 3$ , PRPP-DCM performs better than DCM without precoding by about 8 dB at  $10^{-3}$  BER. The ODP-DCM schemes performs better than the PRPP-DCM scheme with  $p = 3$ . The performance of PRPP-DCM is still impressive because, unlike ODP-DCM which requires CSIT, PRPP-DCM does not require any CSIT.

Also, in Fig. 8, we present the BER performance of PRPP-QCM for the case of 4-QAM ( $p = 2, 4$ ) and 16-QAM ( $p = 2, 3$ ) and  $d_{tx} = 0.1\text{m}$ . The performance of QCM without precoding is also plotted for comparison. It is observed that PRPP-QCM with  $p = 4$  and 4-QAM has an SNR gain of about 20 dB at  $10^{-2}$  BER and about 8.5 dB at  $10^{-4}$  BER compared to QCM without precoding. Also, PRPP-QCM with  $p = 3$  and 16-QAM outperforms QCM by about 12 dB at  $10^{-2}$  BER and about 3 dB at  $10^{-4}$  BER. When compared to PRPP-DCM with 16-QAM, PRPP-QCM with 16-QAM is

better by 5 dB at  $10^{-2}$  BER.

Finally, the effect of varying  $d_{tx}$  on the performance of PRPP-QCM and PRPP-DCM is illustrated in Fig. 9 for the case of 16-QAM,  $p = 3$ , and  $E_b/N_0 = 26$  dB. Here again, we see that the PRPP-DCM and PRPP-QCM perform significantly better than DCM and QCM, respectively. Also, while DCM without precoding performs better than QCM without precoding, with the proposed PRPP precoding QCM performs better.

### V. CONCLUSIONS

We proposed two efficient precoding schemes suited for point-to-point MIMO VLC systems that employ the state-of-the-art DCM and QCM schemes. The first scheme suited for DCM is a weighted diagonal precoding scheme. We optimized the weight by maximizing the minimum distance of the received signal set. This essentially minimized the BER in the high SNR regime. Simulation results showed that the optimized precoding scheme achieved significantly better performance even for small separation between the LEDs ( $d_{tx}$ ). We also proposed a precoding scheme that used a pseudo-random phase matrix as the precoder matrix. This scheme has the advantage of good performance without the need for CSIT. Low-complexity detection methods for large precoder sizes (large values of  $p$ ) is an interesting topic for further research.

### REFERENCES

- [1] P. H. Pathak et al., "Visible light communication, networking, and sensing: a survey, potential and challenges," *IEEE Commun. Surveys & Tutorials*, vol. 17, no. 4, pp. 2047-2077, 4th quarter 2015.
- [2] D. O'Brien, "Visible light communications: challenges and potential," *Proc. IEEE Photon. Conf.*, pp. 365-366, Oct. 2011.
- [3] N. A. Tran et al., "Performance analysis of indoor MIMO visible light communication systems," *Proc. IEEE ICCE'2014*, pp. 60-64, Jul. 2014.
- [4] T. Fath and H. Haas, "Performance comparison of MIMO techniques for optical wireless communications in indoor environments," *IEEE Trans. Commun.*, vol. 61, no. 2, pp. 733-742, Feb. 2013.
- [5] Y. Gong, L. Ding, Y. He, H. Zhu, and Y. Wang, "Analysis of space shift keying modulation applied to visible light communications," *Proc. IETICT'2013*, pp. 503-507, Apr. 2013.
- [6] R. Mesleh et al., "Indoor MIMO optical wireless communication using spatial modulation," *Proc. IEEE ICC'2010*, pp. 1-5, May 2010.
- [7] S. P. Alaka, T. Lakshmi Narasimhan, and A. Chockalingam, "Generalized spatial modulation in indoor wireless visible light communication," *Proc. IEEE GLOBECOM'2015*, Dec. 2015.
- [8] J. Armstrong, "OFDM for optical communications," *J. Lightwave Tech.*, vol. 27, no. 3, pp. 189-204, Feb. 2009.
- [9] R. Tejaswi, T. Lakshmi Narasimhan, and A. Chockalingam, "Quad-LED complex modulation (QCM) for visible light wireless communication," *Proc. IEEE WCNC'2016*, Apr. 2016.
- [10] T. Lakshmi Narasimhan, R. Tejaswi, and A. Chockalingam, "Quad-LED and dual-LED complex modulation for visible light communication," arXiv:1510.08805v3 [cs.IT] 24 Jul 2016.
- [11] L. Zeng et al., "High data rate multiple input multiple output (MIMO) optical wireless communications using white LED lighting," *IEEE J. Sel. Areas Commun.*, vol. 27, no. 9, pp. 1654-1662, Dec. 2009.
- [12] T. Q. Wang et al., "Analysis of an optical wireless receiver using a hemispherical lens with application in MIMO visible light communications," *J. Lightwave Tech.*, vol. 31, no. 11, pp. 1744-1754, Jun. 2013.
- [13] T. V. Pham, H. Le-Minh, and A. T. Pham, "Multi-user visible light communication broadcast channels with zero-forcing precoding," *IEEE Trans. Commun.*, vol. 65, no. 6, pp. 2509-2521, Jun. 2017.
- [14] H. Sifaou et al., "Optimal linear precoding for indoor visible light communication system," *Proc. IEEE ICC'2017*, May 2017.
- [15] J. Barry, J. Kahn, W. Krause, E. Lee, and D. Messerschmitt, "Simulation of multipath impulse response for indoor wireless optical channels," *IEEE J. Sel. Areas in Commun.*, vol. 11, no. 3, pp. 367-379, Apr. 1993.
- [16] T. Lakshmi Narasimhan, Y. Naresh, T. Datta, and A. Chockalingam, "Pseudo-random phase precoded spatial modulation and precoder index modulation," *Proc. IEEE GLOBECOM'2014*, Dec. 2014.